Application of geophysical techniques to support geological mapping projects

Beatriz Benjumea[1*], Anna Gabàs[1], Albert Macau[1], Sara Figueras[1] and Fabian Bellmunt[1] show how the integration of geophysical datasets may improve geological mapping projects.

Better and more detailed information on the bedrock and near-surface geology is needed to assist geological risk assessments, efficient use of water resources or management of rapidly growing regions. Since 2007, the Cartographic and Geological Institute of Catalonia (ICGC) has developed a geological mapping programme, which includes information related to hydrogeology, urban geology or geological risks among others. Within this framework, geophysical techniques make an important contribution refining geological mapping by adding subsoil information to traditional geological data. In this work, we present two studies carried out by ICGC in order to map bedrock geometry or to characterize near-surface sediments in areas with scarce borehole information. The first example of this support focuses on the combination of passive and active geophysical techniques in order to image the Quaternary/Neogene boundary, the bedrock top and to locate faults or the geological map of the Girona urban area (NE of Spain). The second case study shows the potential of reprocessing vintage seismic oil datasets to increase knowledge of the near-surface geological structure in a Neogene Basin located north of Girona (Empordà Basin). The reprocessed seismic reflection image of the first km depth has been interpreted using the refraction velocity model and passive seismic information as constraints. The main objectives are to recover bedrock geometry and structure as well as fault imaging, which are critical for geological mapping projects. The common pattern of the methodologies applied to each case is the integration of different geophysical datasets and the use of both active and passive techniques.

Case 1 — Girona urban geological map

The geophysical survey was designed for two different targets: Quaternary/Neogene contact (shallow study) and bedrock geometry (deep study) in the surroundings of Girona city (Figure 1). Geologically, the studied area is located at the most northern part of the 'La Selva' basin that was related to the opening of the SW Mediterranean Sea during the

Figure 1 *Map of the study area (Girona case study) and location of geophysical profiles and MT, CSAMT and H/V stations. UTM coordinates ED50 Zone 31.*

[1] *Institut Cartogràfic i Geològic de Catalunya, Parc de Montjüic, 08038 Barcelona, Spain.*
[*] *Corresponding author, E-mail: beatriz.benjumea@icgc.cat*

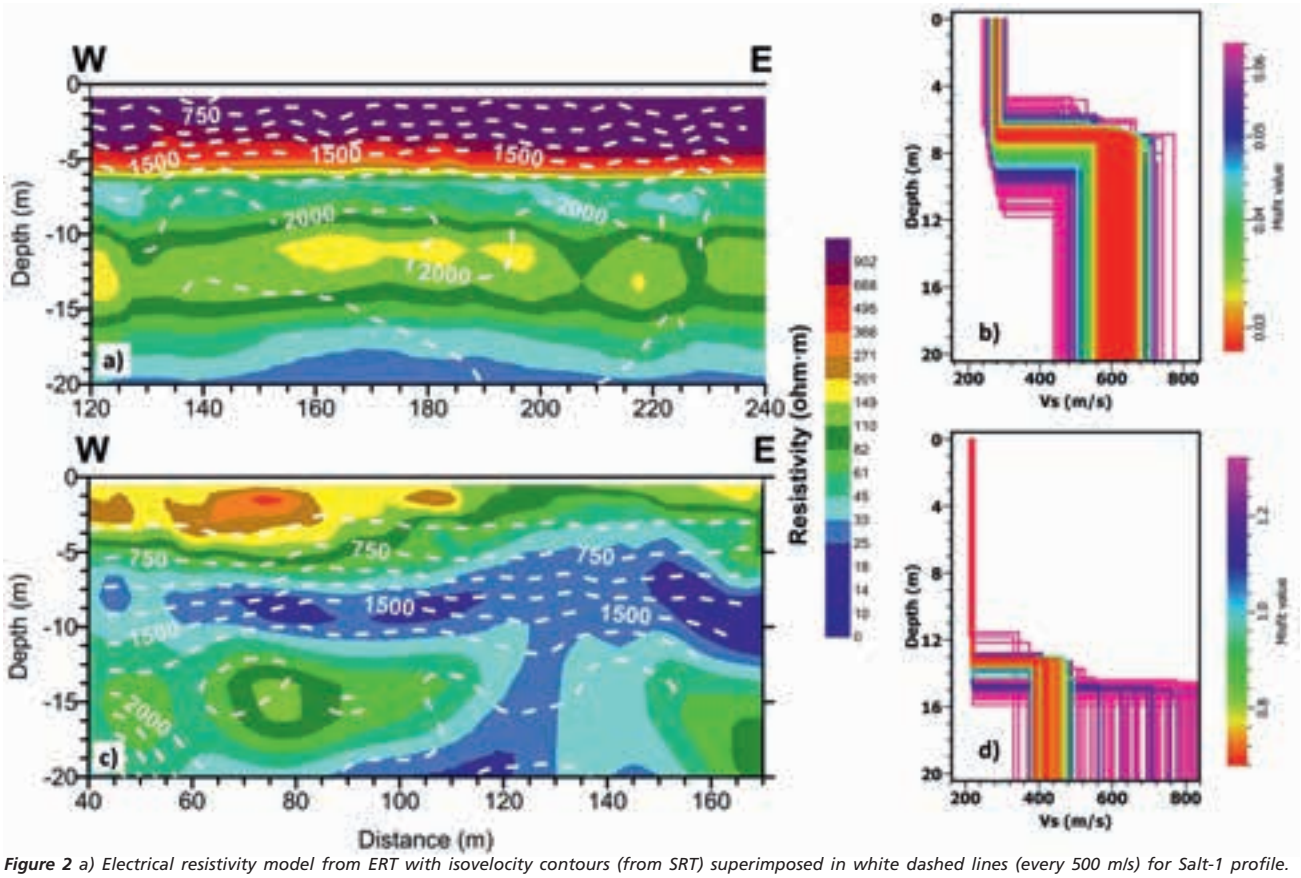

Figure 2 *a) Electrical resistivity model from ERT with isovelocity contours (from SRT) superimposed in white dashed lines (every 500 m/s) for Salt-1 profile. b) Shear-wave velocity models from surface analysis corresponding to a shot gather of Salt-1 profile. Misfit error is colour coded.c) and d) same as a) and b) respectively for Salt-3 profile.*

Neogene. In this area, the basin is infilled by Neogene and Quaternary unconsolidated detrital sediments derived from the erosion of the surrounding reliefs. The deposits overlay a complex basement composed by Paleozoic metamorphic and igneous rocks; and Paleogene sedimentary rocks (IGC, 1997-2009).

The methodology included the combination of seismic refraction (SRT) and electrical resistivity tomography (ERT) supported by shear-wave velocity for the shallow study. Three collocated ERT and SRT profiles have been carried out to test the suitability of the combination of both techniques to distinguish between Quaternary and Neogene sediments in this area. On the other hand, the integration of active (control source audiomagnetotellurics method-CSAMT) and passive techniques (H/V microtremor method and Magnetotellurics –MT method) were used to image the basin and to distinguish between bedrock lithologies in the deep study. From these geophysical methods, the analysis of the H/V spectral ratio of microtremors is a technique borrowed from earthquake engineering that has been applied to geophysical exploration studies in the last few years (e.g. Ibs-von Seht and Wohlenberg 1999; Delgado et al., 2000; Benjumea et al., 2011). Using the microtremor measurement at a single three component seismic station provides the soil fundamental frequency than can be related to bedrock depth through Vs information or empirical relationships as we will discuss in the two case studies shown in this paper.

Shallow study — Combination of electrical resistivity tomography and seismic methods

Seismic datasets were acquired using 48 10 Hz vertical geophones linearly spaced every 2.5 m. Eleven shot positions were distributed along the geophone array. The seismic velocity model was obtained using refraction tomography. The surface waves of seismic records corresponding to shots located out of the array have been analysed in order to obtain a 1D shear-wave velocity model. This information can constrain the interpretation of the P-wave velocity models. ERT data were acquired with 72 electrodes using 5 and 3 m electrode spacing depending on the profile. Datasets with both Wenner-Schlumberger and dipole-dipole array configurations were acquired.

Figure 2 shows the comparison between the results obtained for Salt-1 and Salt-3 profiles. Electrical resistivity is shown in a colour coded graphic overlapped with isovelocity contours from the seismic model. Different electrical

characteristics can be observed in these two profiles. The Salt-1 profile shows a sharp electrical resistivity contrast at around 6 m from values higher than 600 ohm·m to 60-80 ohm·m (Figure 2a). Figure 2c shows three layers in Salt-3 profile: two medium resistive zones separated by a more conductive one. Regarding the P-wave velocity information, slow velocity materials (<1500 m/s) appears to be thicker in Salt-3 (10-12 m depth) than in Salt-1 (around 6 m). As a first approach, the high resistivity values and the low P-wave velocities of Salt-1 can be assigned to Quaternary sediments. However, the change at 6 m depth in both seismic and electrical resistivity values could also be related to a water saturation increase causing a decrease of electrical resistivity and a change of P-wave velocity to approx. 1500 m/s. To discern the origin of the sharp contrast, we retrieved shear-wave velocity from surface wave analysis. The shear-wave velocity model shown in Figure 2b depicts a significant change (2 to 2.5 of velocity contrast) at 6 m approximately. Since shear-wave velocity is not affected by the degree of water saturation, this sharp Vs increment confirms that both resistivity and P-wave velocity models contrasting at that depth correspond to a lithological change interpreted as the Quaternary-Neogene boundary (gravels over lutites according to the resistivity values). The use of shear-wave velocity information also constrained the interpretation of the Salt-3 profile. In this case, the change from conductive to medium resistive zone at around 12 m depth coincides with a change of P-wave velocities that increase to values higher than 1500 m/s (Figure 2c). The main change in the Vs profile is located at around 12 m depth interpreted as the Quaternary-Neogene boundary (Figure 2d). In this profile, Quaternary sediments are related to a sandy over a clayey layer considering the resistivity values. Neogene material is interpreted as lutites like in the Salt-1 profile.

Deep study — Combination of CSAMT-MT method with H/V microtremor technique

The second study in this area was focused in imaging the bottom of Neogene sediments. In this case, electrical resistivity models were obtained combining active (control source audiomagnetotellurics method) and passive measurements (magnetotellurics method). In order to obtain another constraint from the sediment/bedrock contact, H/V measurements were performed.

A total of 87 seismic noise stations were distributed along three profiles in the study area (Figure 1). These datasets were acquired using a six-channel Cityshark datalogger and 2 Lennartz 0.2 Hz LE-3D 3C sensors. The CSAMT and MT data acquisition was performed at 21 stations along two profiles (Figure 1). MT stations consisted of ADU07 (Metronix) system (128-4096 Hz). The Geometrics Stratagem EH4 system with an artificial EM signal (10-92000 Hz) was used for CSAMT method. We will focus on one of the profiles that cross the study area from SW to NE.

Figure 3 shows the resistivity model for Transversal South profile obtained from a combination of CSAMT and MT data. This model exhibits three distinct zones. A near-surface conductive layer (1-100 Ω·m) is presented in the whole profile with a variable depth from surface at the SW end up to a maximum of 450 m at the middle of the profile. This zone has been interpreted as Neogene materials (clays, sands and gravel levels). Some isolated resistive bodies (400-600 Ω·m) within this layer mark the presence of the sandy-gravel zones. The second distinct zone is characterized by resistivity

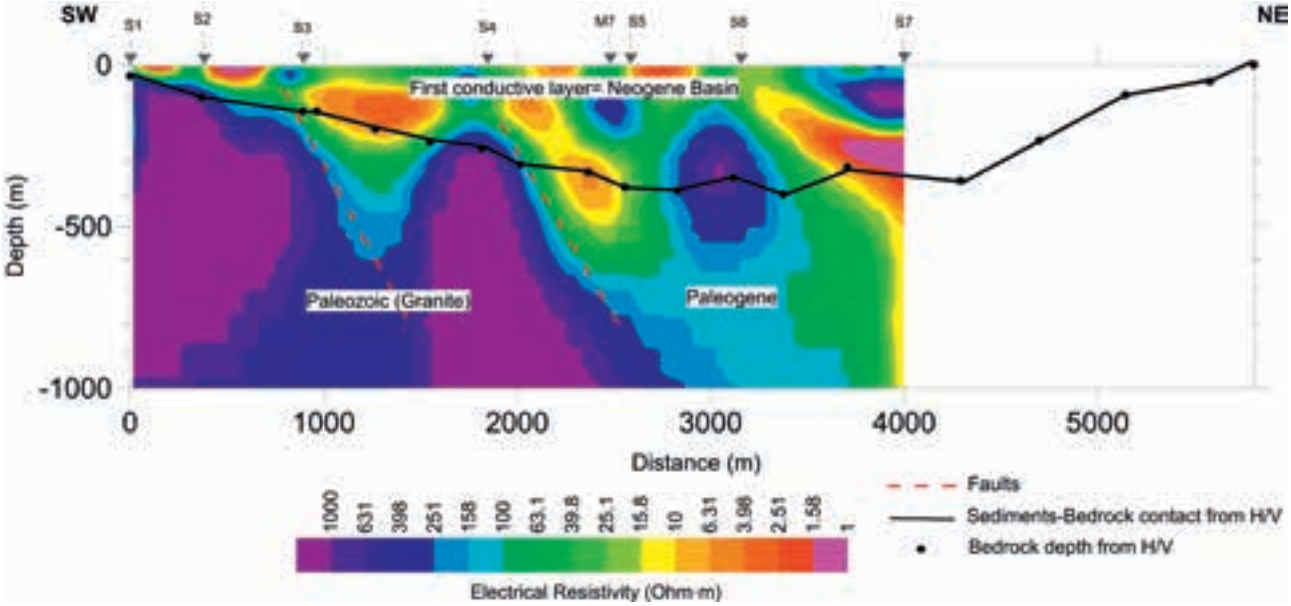

Figure 3 *Two-dimensional CSAMT and MT resistivity model along the Transversal South survey line. Black dots mark bedrock depth obtained from fH/V-depth empirical relationship (Ibs-Von Seht and Wolhenberg S/R, 1999). Modified from Gabàs et al., 2014.*

values ranging between 100 and 400 Ω·m located at the NE part of the model below 500 m depth. This middle resistive structure corresponds to Paleogene materials consisting of sandstones, marls, conglomerates and lutites. Finally, a zone characterized by resistive materials (600-1000 Ω·m) can be found close to the surface in the SW part of the model, reaching a depth of 1000 m at around 3000 m distance. These high resistivity values can be interpreted as Paleozoic granitic materials. Hence, in this SW end of the profile, the sharp electrical change between the first layer and this very resistive zone has been interpreted as the Neogene sediments-Paleozoic bedrock contact and has been clearly imaged with the resistivity model itself. In addition, lateral changes of the electrical resistivity model help to define the signature of faults not observable from the surface. However, at the NE part of the profile, the vertical electrical changes are smoother and the delineation of bedrock top is difficult using only the resistivity model because of the similar electrical characteristics of Neogene-Paleogene materials. We have included the results from the H/V microtremor measurements to solve the uncertainties. In this study area, the contact between overburden (Neogene) and bedrock (Paleogene or Paleozoic) has been considered as the cause of the soil resonance owing to significant contrast of seismic properties between them. The black dots shown in Figure 3 mark the bedrock depth obtained from the fundamental frequency values. In this case, an empirical relationship proposed by Ibs-Von Seht and Wolhenberg (1999) has been used. Although this relationship was obtained from measurements in the western Lower Rhine Embayment (Germany), array measurements in Girona area confirmed the validity of this relationship in the study area (Gabàs et al., 2014). These bedrock depth values are coherent with the electrical resistivity changes at the SW end of the profile and help to define the bottom of the Neogene Basin at the NE sector where sediments are in contact with Paleogene rocks with a similar electrical signature.

Case 2 — Geological map of the Empordà Basin

The Empordà Basin is located between the Pyrenees, the Catalan Coastal Range (CCR) and the Mediterranean Sea (Figure 4). Its formation and structure is relatively complex and is due to extensional movements within the Alpine orogeny, ranging from the Oligocene to the present. A fault system NW-SE is the determinant of the horsts and grabens structure of the basin (Fleta et al., 1991). The basin is filled by Miocene and Pliocene continental and marine deposits. The Pliocene sequence unconformably overlies the Miocene deposits. These Neogene materials lay upon bedrock which is composed of Palaeozoic metamorphic and plutonic rocks, Mesozoic limestones and Paleogene rocks.

This basin was the target of several oil companies during the 1980s and from that time, several seismic reflection datasets are available. The objective of those 2D seismic lines was to image deep geological structures for exploration purposes. In this paper, we present the result of reprocessing one of these lines focusing on the near-surface to image the Neogene basin structure and to characterize different bedrock units. The dataset used in this study was part of the S29 line that was acquired with only 48 channels leading to a low-fold dataset. The seismic data was reprocessed using a reflection processing flow that included: first break picking and removal, maximum offset of 750 m, reducing trace length to 1.5 s, refraction statics, band-pass filtering (10-90 Hz), spectral whitening to reduce surface wave noise, velocity analysis, NMO-Stack and F-X Deconvolution. Migration tests did not improve the final image owing to low signal-to-noise ratio.

Figure 4 *Orthophoto map of the study area. Orange line shows the location of seismic profile included in this study.*

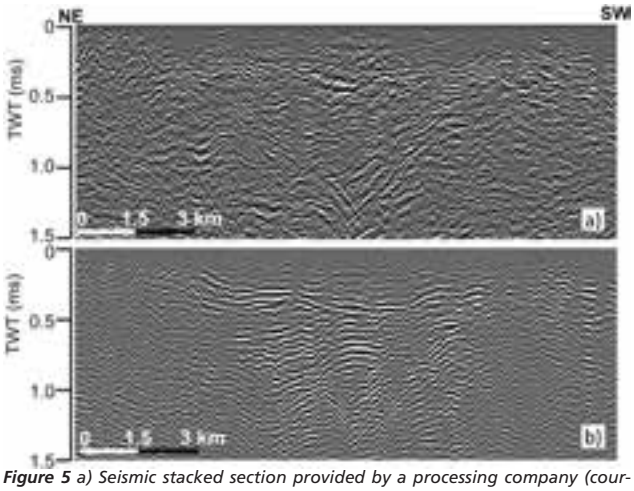

Figure 5 *a) Seismic stacked section provided by a processing company (courtesy of CEPSA) b) Stacked section resulting from reprocessing summarized in the text.*

This processing flow was focused on near-surface imaging as can be seen in the comparison between the original processing and this new one (Figure 5). In spite of the low-fold image, several reflections can be observed in the new stack that were not imaged with the original processing. In order to constrain the interpretation of this image, two other sources of information were used. First, a P-wave velocity model was obtained from seismic refraction tomography using first arrival travel times. Second, new seismic noise measurements were carried out with a 3C component sensor to obtain a set of soil fundamental frequencies. Forty one seismic stations were distributed along the location of the vintage seismic line.

In this case, the assessment of the bedrock depth from the soil fundamental frequencies was done using a local empirical relationship calculated by ICGC at three Neogene basins in north-east Spain. The relationship is the result of fitting bedrock depth estimated from shear-wave velocity profiles from array measurements and the corresponding H/V frequency (Gabàs et al., 2016).

Figure 6b shows the P-wave velocity model obtained from seismic refraction tomography. We have included a sector of the 1:50.000 geological map in Figure 6a to help with interpretation. Several faults were inferred from geological information and are plotted as a discontinuous line. P-wave velocity values range from 1000 to more than 5000 m/s. The high-velocity distribution reflects the bedrock geometry, shallow bedrock is identified in the NE sector of the profile and the maximum depth is detected at around 8000 m distance. The strong lateral contrast observed between 4500 and 5500 m distance would correspond to the fault indicated in the geological map. Delineation of the Neogene base with the tomographic model is not straightforward owing to the smooth character of the tomograms. The use of the velocity gradient can help to divide the velocity model into sediments and rock domains. We have chosen the isovelocity contours that lie in the velocity range corresponding to the maximum velocity gradient as indicators of the basin base (3500 to 4000 m/s). Figure 6c shows these isovelocity contours superimposed to the reflection stacked section (dashed orange lines) after transforming the velocity model from depth to two-way traveltime. In addition, bedrock location from H/V measurements in ms has been calculated using the velocity model. The result is also shown in Figure 6c as yellow diamonds. By comparing the stacked section with both isovelocity contours and H/V results we observe a good agreement between these markers and a dipping reflection to the NE of the line between 6500 to 12.000 m distance. This is interpreted as the Neogene base (Figure 6d). Hence, the reflective zone above this base could be related to the Pliocene Base. The transparent zone in the north-east part of the line would correspond to the Paleozoic bedrock, which is confirmed by the high-velocity values in the tomogram. Below the dipping reflector, several structures can be observed that may correspond to Mesozoic limestones. Different reflection character reveals a lithological change in bedrock along the profile that would not be possible to assess with the other methods.

Conclusions

The two case studies presented in this paper highlight the potential of combining different geophysical datasets to provide new insights into the geological interpretation especially since borehole information is scarce. In both cases, the methodology including both active and passive techniques has been designed according to the investigation depth and the previous available datasets. Regarding the second case study, this paper reinforces the importance of reprocessing vintage data to retrieve new information at a different scale to the original.

In the shallow study carried out in the Girona area, a combination of electrical resistivity and seismic tomography is suited to identifying interesting contacts for urban geological mapping such as the Quaternary base. However, the use of surface waves for Vs retrieval as a byproduct of the seismic refraction survey helps to discern if the P-wave or electrical resistivity changes can be related with a lithological contact or the presence of fluid.

The two Neogene basins have been the subject of deeper studies within the geological mapping project. In the Girona basin, the electrical resistivity model from CSAMT and MT techniques images faults and changes in bedrock lithology. In the case where the electrical signature of sediments and rock is different, the model provides the contact between Neogene sediments and Paleozoic rock. However, if the sediments overlie Paleogene rock, the similar resistivity values preclude delineation of the basin base. H/V measurements help to divide the geophysical model into sedimentary and bedrock subdomains based on the strong acoustic impedance contrast between them. Finally, the second Neogene basin has been

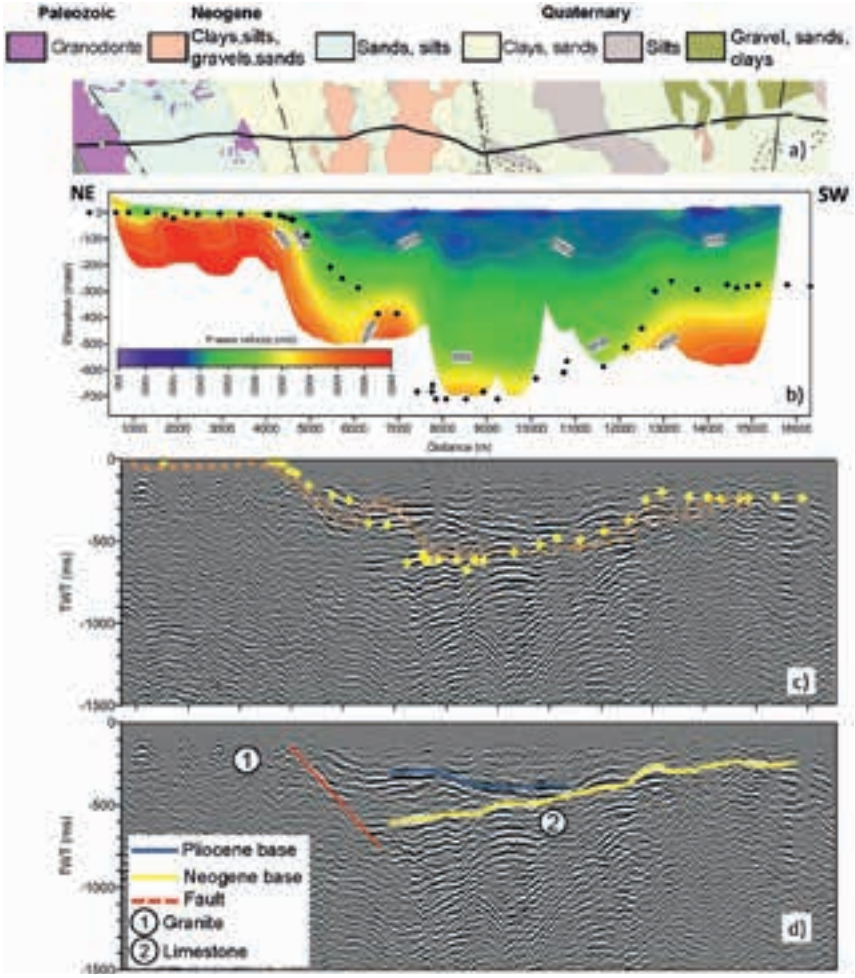

Figure 6 *a) Sector of the geological map of the Empordà Basin corresponding to the location of the S29 seismic profile (www.icgc.cat). b) P-wave velocity model obtained from seismic refraction tomography. Black diamonds indicate the bedrock depth provided by the H/V technique. c) Seismic stacked section. Dashed orange lines correspond to 3500 to 4000 m/s isovelocity contours from b). Yellow diamonds are the H/V result shown in b) converted to twt in ms. d) Interpretation of the seismic stacked section generated from the synthesis of the results from seismic refraction, reflection and H/V methods.*

studied by reprocessing seismic vintage datasets. In spite of low-fold and data acquisition parameters designed for deeper studies, a processing flow focused on the near-surface is suitable for highlighting reflections otherwise hidden in the original processing. To complement the structural pattern deduced from the reflection image, refraction tomograms – another byproduct from the reprocessing – and new H/V measurements have been used. These complementary datasets help to distinguish which reflection corresponds to the Neogene base.

Acknowledgments

The authors would like to acknowledge the students who collaborated during the fieldwork. We would like to thank Mariona Esquerda and Esther Falgàs for their help during data acquisition. We wish to thank Miquel Vilà and Xavier Berastegui for their input regarding the geology of the study areas. We thank Jorge Navarro from CEPSA for providing the seismic reflection data from the Empordà basin.

References

Benjumea, B., Macau, A., Gabàs, A., Bellmunt, F., Figueras, S. and Cirés, J. [2011]. Integrated geophysical profiles and H/V microtremor measurements for subsoil characterization. *Near Surface Geophysics*, **9** (5), 413-425.

Delgado, J., López Casado, C., Giner, J., Estévez, A., Cuenca, A. and Molina, S. [2000]. Microtremors as a geophysical exploration tool: Applications and limitations. *Pure and Applied Geophysics*, **157**, 1445–1462.

Fleta, J., Arasa, A. and Escuer, J. [1991]. El Neógeno del Empordà y Baix Ebre (Catalunya): estudio comparativo. *Acta geológica hispánica*, **26** (3), 159-171.

Gabàs, A., Macau, A., Benjumea, B., Bellmunt, F., Figueras, S. and Vilà, M. [2014]. Combination of geophysical methods to support urban geological mapping. *Surveys in Geophysics*, **35** (4), 983-1002.

Gabàs, A., Macau, A., Benjumea, B., Queralt, P., Ledo, J., Figueras, S., and Marcuello, A. [2016]. Joint Audio-Magnetotelluric and Passive Seismic Imaging of the Cerdanya Basin. *Surveys in Geophysics*, 1-25, http://dx.doi.org/10.1007/s10712-016-9372-4.

Ibs-von Seht, M. and Wohlenberg, J. [1999]. Microtremor measurements used to map thickness of soft sediments. *Bulletin of Seismological Society of America*, **89**, 250–259.

IGC [2003–2009]. *Mapa geològic de Catalunya 1:25000*, (sheet 332 2-1), accessed at: http://www.icgc.cat.